

# UC Riverside

## UC Riverside Previously Published Works

### Title

Complex Interplay Among Nuclear Receptor Ligands, Cytosine Methylation, and the Metabolome in Driving Tris(1,3-dichloro-2-propyl)phosphate-Induced Epiboly Defects in Zebrafish

### Permalink

<https://escholarship.org/uc/item/7364k3nz>

### Journal

Environmental Science and Technology, 53(17)

### ISSN

0013-936X

### Authors

Dasgupta, Subham  
Vliet, Sara MF  
Cheng, Vanessa  
et al.

### Publication Date

2019-09-03

### DOI

10.1021/acs.est.9b04127

Peer reviewed



# HHS Public Access

Author manuscript

*Environ Sci Technol.* Author manuscript; available in PMC 2020 September 03.

Published in final edited form as:

*Environ Sci Technol.* 2019 September 03; 53(17): 10497–10505. doi:10.1021/acs.est.9b04127.

## Complex Interplay Among Nuclear Receptor Ligands, Cytosine Methylation, and the Metabolome in Driving Tris(1,3-Dichloro-2-Propyl) Phosphate-Induced Epiboly Defects in Zebrafish

Subham Dasgupta<sup>†</sup>, Sara M. F. Vliet<sup>†</sup>, Vanessa Cheng<sup>†</sup>, Constance A. Mitchell<sup>†</sup>, Jay Kirkwood<sup>‡</sup>, Alyssa Vollaro<sup>‡</sup>, Manhoi Hur<sup>‡</sup>, Chris Mehdizadeh<sup>†</sup>, David C. Volz<sup>†,\*</sup>

<sup>†</sup>Department of Environmental Sciences, University of California, Riverside, California 92521, United States

<sup>‡</sup>Metabolomics Core Facility, Institute for Integrative Genome Biology, University of California, Riverside, California 92521, United States

### Abstract

Tris(1,3-dichloro-2-propyl) phosphate (TDCIPP) is a high-production volume organophosphate flame retardant (OPFR) that induces epiboly defects during zebrafish embryogenesis, leading to disruption of dorsoventral patterning. Therefore, the objectives of this study were to 1) identify potential mechanisms involved in TDCIPP-induced epiboly defects and 2) determine whether co-exposure to triphenyl phosphate (TPHP) – an OPFR commonly detected with TDCIPP – enhances or mitigates epiboly defects. While TDCIPP-induced epiboly defects were not associated with adverse impacts on cytoskeletal protein abundance *in situ*, co-exposure of embryos to TPHP partially blocked TDCIPP-induced epiboly defects. As nuclear receptors are targets for both TPHP and TDCIPP, we exposed embryos to TDCIPP in the presence or absence of 69 nuclear receptor ligands and, similar to TPHP, found that ciglitazone (a peroxisome proliferator-activated receptor  $\gamma$  agonist) and 17 $\beta$ -estradiol (E2; an estrogen receptor  $\alpha$  agonist) nearly abolished TDCIPP-induced epiboly defects. Moreover, E2 and ciglitazone mitigated TDCIPP-induced effects on CpG hypomethylation within target loci prior to epiboly, and ciglitazone altered TDCIPP-induced effects on the abundance of two polar metabolites (acetylcarnitine and CDP-choline) during

\*Phone: (951) 827-4450; Fax: (951) 827-4652; david.volz@ucr.edu.

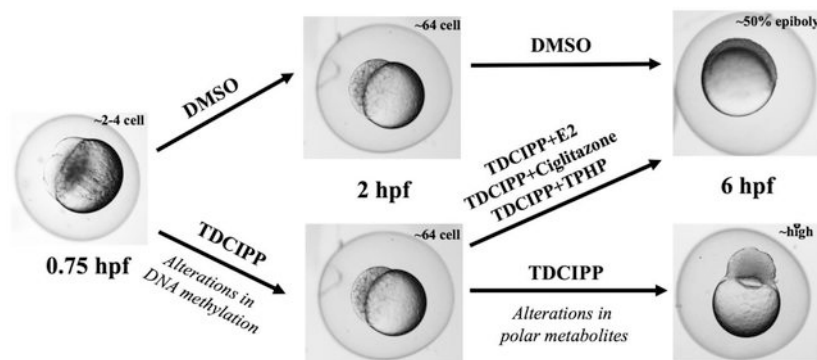
#### Supporting Information

A Microsoft Excel spreadsheet containing 1) BSAS-specific information and output; 2) data extracted from the U.S. EPA's ToxCast dashboard; 3) information and data for nuclear receptor ligand screening; and 4) raw data for metabolomics is provided as Supplemental File 1 (Tables S1–S9). Supplemental File 2 contains Figures S1–S4 as well as additional details for analysis of polar and non-polar metabolites. This information is available free of charge via the Internet at <http://pubs.acs.org>. The authors declare no competing financial interest.

**Publisher's Disclaimer:** "Just Accepted" manuscripts have been peer-reviewed and accepted for publication. They are posted online prior to technical editing, formatting for publication and author proofing. The American Chemical Society provides "Just Accepted" as a service to the research community to expedite the dissemination of scientific material as soon as possible after acceptance. "Just Accepted" manuscripts appear in full in PDF format accompanied by an HTML abstract. "Just Accepted" manuscripts have been fully peer reviewed, but should not be considered the official version of record. They are citable by the Digital Object Identifier (DOI®). "Just Accepted" is an optional service offered to authors. Therefore, the "Just Accepted" Web site may not include all articles that will be published in the journal. After a manuscript is technically edited and formatted, it will be removed from the "Just Accepted" Web site and published as an ASAP article. Note that technical editing may introduce minor changes to the manuscript text and/or graphics which could affect content, and all legal disclaimers and ethical guidelines that apply to the journal pertain. ACS cannot be held responsible for errors or consequences arising from the use of information contained in these "Just Accepted" manuscripts.

epiboly. Overall, our results point to a complex interplay among nuclear receptor ligands, cytosine methylation, and the metabolome in both the induction and mitigation of epiboly defects induced by TDCIPP.

## Graphical Abstract



## Introduction

Tris(1,3-dichloro-2-propyl) phosphate (TDCIPP) is a high-production volume organophosphate flame retardant (OPFR) used around the world,<sup>1</sup> and its use and human exposure within the United States have increased over the last decade.<sup>2</sup> Consequently, elevated levels of bis(1,3-dichloro-2-propyl) phosphate (BDCIPP) – the primary metabolite of TDCIPP in mammals – have been detected within human populations, including pregnant mothers<sup>3</sup>, mother-toddler pairs<sup>4</sup>, and more recently, human placental samples.<sup>5</sup> Moreover, TDCIPP and BDCIPP have been associated with abnormal pregnancy outcomes,<sup>6,7</sup> highlighting the importance of further understanding the potential impacts of TDCIPP on early development.

During gastrulation within certain animals, epiboly is a key developmental event that, through coordinated cell movements, leads to cell layer thinning and spreading, organization of cells into germ layers, and formation of the body axis.<sup>8</sup> In zebrafish, epiboly progression is regulated by a complex, highly regulated interplay among cytoskeletal reorganization, zygotic genome activation, and developmental signaling pathways,<sup>8</sup> leading to dorsoventral patterning and organogenesis later in development. Therefore, epiboly disruption by environmental contaminants can result in a cascade of defects that have the potential to irreversibly alter the normal trajectory of development. Using zebrafish as a model, previous studies have reported that TDCIPP disrupts epibolic movements during embryonic development.<sup>9–12</sup> These epiboly defects subsequently lead to an array of downstream abnormalities during embryogenesis,<sup>10</sup> underscoring the importance of epiboly as a potential target for embryonic exposure to chemicals.

Actin and tubulin provide the cytoskeletal foundation for microfilament and microtubule networks, respectively, that drive epibolic movements within gastrulating embryos. Exposure of zebrafish embryos to cytochalasin B and nocodazole – potent inhibitors of actin and tubulin polymerization, respectively – results in epiboly delay or arrest.<sup>13–14</sup> However, the

impacts of TDCIPP on cytoskeletal reorganization have not yet been studied. Coordination of cell movements during epiboly are also regulated by both maternal and zygotic transcription, and epiboly initiation and progression are regulated by maternal and zygotic factors, respectively.<sup>8</sup> However, we showed that TDCIPP did not delay the maternal-to-zygotic transition (MZT) nor affect mRNA levels of maternal or zygotic factors.<sup>10</sup> Despite a 9- to 20-fold decrease in mRNA levels of *sizzled (szl)* – a bone morphogenetic protein (BMP) pathway gene that regulates dorsoventral patterning – within TDCIPP-treated embryos, mRNA-sequencing data also revealed minimal impacts on BMP pathway-related transcripts.<sup>9,10</sup> In addition, prior to epiboly, TDCIPP exposure from 0.75–2 h post-fertilization (hpf) resulted in genome-wide CpG hypomethylation at 2 hpf,<sup>11,15</sup> but co-exposure with a methyl donor (folic acid) did not mitigate TDCIPP-induced CpG hypomethylation nor epiboly defects.<sup>11</sup> Therefore, despite our prior transcriptomic and epigenetic studies, no clear target nor mechanism underlying TDCIPP-induced epiboly defects has emerged based on our findings to date.

Within this study, we initially studied the effects of triphenyl phosphate (TPHP) – another high-production volume OPFR commonly found at elevated levels with TDCIPP – on TDCIPP-induced epiboly defects and used these data to segue into investigating other potential targets for TDCIPP during early embryonic development. As OPFR mixtures are found within environmental media, there is a potential for maternal and prenatal embryonic exposure to mixtures of OPFRs and their corresponding metabolites.<sup>1,2,7,16</sup> Previous studies have shown that mixtures of flame retardants and corresponding metabolites lead to additive or synergistic toxic effects.<sup>17,18</sup> However, the potential impacts of OPFR mixtures during early development have not been studied. Based on these knowledge gaps, the objectives of this study were to 1) investigate whether TPHP enhances or mitigates TDCIPP-induced epiboly defects; 2) leverage the U.S. Environmental Protection Agency's (EPA's) ToxCast data as well as in-house high-content screening to identify lead compounds that may enhance or mitigate TDCIPP-induced epiboly defects; and 3) rely on these lead compounds as pharmacologic tools to determine whether potential effects on cytoskeletal reorganization as well as DNA methylation and the embryonic metabolome are associated with TDCIPP-induced epiboly defects.

## Methods

### Animals

Adult wild-type (5D) zebrafish were maintained and bred on a recirculating system using previously described procedures.<sup>19</sup> Adult breeders were handled and treated in accordance with Institutional Animal Care and Use Committee (IACUC)-approved animal use protocols (#20150035 and #20180063) at the University of California, Riverside.

### Chemicals

TDCIPP (99% purity; CAS#: 13674-87-8) and TPHP (99.5% purity; CAS#: 115-86-6) were purchased from ChemService, Inc. (West Chester, PA); diphenyl phosphate (DHP, >99% purity; CAS#: 53306-54-0), 17 $\beta$ -estradiol (E2, 98% purity; CAS#: 50-28-2), 17 $\alpha$ -ethinylestradiol (EE2, 98% purity; CAS#: 47-63-6), genistein (98% purity; CAS#:

446-72-0), cytochalasin B (98% purity; CAS#: 14930-96-2), and nocodazole (99% purity; CAS#: 31430-18-9) were purchased from Millipore Sigma (Burlington, MA); BDCIPP (95% purity; CAS#: 72236-72-7) was purchased from Toronto Research Chemicals (ON, Canada); and ciglitazone (>99.4% purity; CAS#: 74772-77-3) was purchased from Tocris Bioscience (Bristol, UK). For all chemicals, stock solutions were prepared in high-performance liquid chromatography (HPLC)-grade dimethyl sulfoxide (DMSO) and stored within 2-mL amber glass vials with polytetrafluoroethylene-lined caps. The SCREEN-WELL Nuclear Receptor Ligand Library (100  $\mu$ L of 1 mM or 10 mM stock per compound) was obtained from Enzo Life Sciences, Inc. (Farmingdale, NY) and stored at  $-20^{\circ}\text{C}$ . Working solutions (1:1000 dilutions of stock) were prepared in particulate-free water from our recirculating system (pH and conductivity of  $\sim 7.2$  and  $\sim 950$   $\mu\text{S}$ , respectively) immediately prior to each experiment. Based on our previous findings,<sup>9,10</sup> we selected a TDCIPP concentration (3.12  $\mu\text{M}$ ) that reliably impacted epiboly progression; furthermore, our prior studies have shown that, within the first 2–6 h of embryonic development, TDCIPP uptake is rapid but not metabolized to BDCIPP.<sup>15,20</sup>

### OPFR Co-Exposures

We assessed whether exposure to TDCIPP in the presence or absence of BDCIPP, TPHP, or DPHP (the primary metabolite of TPHP in mammals) resulted in mitigation or enhancement of TDCIPP-induced epiboly defects. For all exposures, the final DMSO concentration across all treatment groups was 0.2%; for single compound exposures, an equivalent volume of DMSO alone was added to working solutions to yield 0.2% DMSO. Embryos were exposed to 0.2% DMSO or 3.12  $\mu\text{M}$  TDCIPP in the presence or absence of 125  $\mu\text{M}$  BDCIPP, 3.12  $\mu\text{M}$  TPHP, or 500  $\mu\text{M}$  DPHP from 0.75 to 6 hpf in clean 60-mm glass petri dishes (one dish per treatment) containing 10 mL of exposure solution and 30 embryos per petri dish. All exposures were conducted under static conditions at  $28^{\circ}\text{C}$  within a temperature-controlled incubator under a 14-h:10-h light:dark cycle. The TPHP concentration was selected based on the maximum tolerated concentration (MTC) for survival, and BDCIPP and DPHP concentrations were selected based on the limit of solubility in system water at room temperature. If co-exposure with BDCIPP, TPHP, or DPHP resulted in mitigation or enhancement of TDCIPP-induced epiboly defects, then exposures were repeated as described above using three replicate petri dishes per treatment and 30 embryos per replicate petri dish. All embryos were imaged for epiboly defects (normal or delayed/arrested) at 6 hpf using a Leica MZ10 F stereomicroscope equipped with a DMC2900 camera. Treatment-specific differences were calculated using a one-way ANOVA followed by Tukey-based multiple comparison procedures within Prism 8 (GraphPad, San Diego, CA).

### Nuclear Receptor Ligand Library Screens

Based on positive hits from OPFR co-exposures, the U.S. EPA's ToxCast dashboard (<https://actor.epa.gov/dashboard/>) was used in order to identify common molecular targets between TDCIPP and TPHP. Data extraction and analysis from the ToxCast dashboard were based on Volz et al. (2015),<sup>21</sup> with a logarithmic half-maximal activity concentration ( $\log \text{AC}_{50}$ ) threshold of 1  $\mu\text{M}$ . Based on these data, we then investigated whether nuclear receptors play a potential role in TDCIPP-induced epiboly defects. Briefly, embryos were exposed from 0.75–6 hpf to 0.2% DMSO or 3.12  $\mu\text{M}$  TDCIPP in the presence or absence of 69

different nuclear receptor ligands provided within Enzo's SCREEN-WELL Nuclear Receptor Ligand Library (Table S1). Initial ligand concentrations were selected using MTCs identified by Mitchell et al. (2018)<sup>22</sup> following a 24–72 hpf exposure, with additional optimization of MTCs if embryonic survival was adversely affected at 6 hpf.

Similar to OPFR co-exposures described above, all ligands were first screened as co-exposures at a single limit concentration using one glass petri dish per treatment and 30 embryos per petri dish and phenotyped at 6 hpf. Based on these results, a subset of ligands was prioritized for additional testing based on the presence of >50% normal embryos and a >140% increase in normal embryos over corresponding TDCIPP-only treatments; these decision criteria were used to account for slight variability of TDCIPP-induced epiboly defects across different embryo clutches and days of screening. For each of these ligands, co-exposures were repeated using three replicate glass petri dishes per treatment and 30 embryos per replicate petri dish. If reproducible effects were observed across replicate petri dishes, co-exposures were conducted with the top two lead compounds in concentration-response format. Additional details of the ligand screen are provided in Figure 2A. All embryos were imaged for epiboly defects (normal or delayed/arrested) at 6 hpf using a Leica MZ10 F stereomicroscope equipped with a DMC2900 camera. Treatment-specific differences were calculated using a one-way ANOVA followed by Tukey-based multiple comparison procedures within Prism 8 (GraphPad, San Diego, CA).

### Pre-Treatment Experiments

Based on co-exposure results, pre-treatment experiments were performed in order to confirm that mitigation of TDCIPP-induced toxicity was not an artifact of decreased uptake of TDCIPP within co-exposure solutions. Briefly, embryos (30 per replicate glass petri dish) were pre-treated with 0.2% DMSO, 3.12  $\mu$ M TPHP, 5  $\mu$ M ciglitazone, or 5  $\mu$ M E2 from 0.75–2 hpf followed by exposure to 0.2% DMSO or 3.12  $\mu$ M TDCIPP from 2–6 hpf in three replicate glass petri dishes per treatment (10 mL of treatment solution per petri dish). All exposures were conducted under static conditions at 28°C within a temperature-controlled incubator under a 14-h:10-h light:dark cycle. All embryos were imaged for epiboly defects (normal or delayed/arrested) at 6 hpf using a Leica MZ10 F stereomicroscope equipped with a DMC2900 camera. Treatment-specific differences were calculated using a one-way ANOVA followed by Tukey-based multiple comparison procedures within Prism 8 (GraphPad, San Diego, CA).

### Cytoskeletal Staining

To assess the potential impacts of TDCIPP on embryonic cytoskeletal proteins (actin and tubulin), embryos were exposed to 0.2% DMSO or 3.12  $\mu$ M TDCIPP from 0.75 to 5 hpf within 1.25-mL glass vials containing one embryo and 333  $\mu$ L of treatment solution per vial (20 vials per treatment). Additionally, 12.5  $\mu$ M cytochalasin B and 12.5  $\mu$ M nocodazole were used as positive controls, and a 2-h exposure period from 3–5 hpf for both positive controls was used since initiation of exposure at 0.75 hpf resulted in 100% mortality (Figure S1). At 5 hpf, live embryos were pooled according to treatment groups and fixed overnight in 4% paraformaldehyde/1X phosphate-buffered saline (PBS). Fixed embryos were incubated with either 1:200 Alexa Fluor 488-conjugated phalloidin (Millipore Sigma), or



1:6.25 6G7 ( $\beta$ -tubulin) IgG1 (Developmental Studies Hybridoma Bank, University of Iowa) followed by incubation with IgG1-specific Alexa Fluor 488-conjugated secondary antibody (Millipore Sigma) following previously described protocols.<sup>10</sup> Embryos were then imaged using a Leica MZ10 F stereomicroscope equipped with a DMC2900 camera and GFP filter. Yolk sac fluorescence for each embryo was quantified within a randomly selected area of the yolk sac using Adobe Photoshop, whereas cell area for each embryo was calculated as the average area across 15 individual cells within the blastomere using ImageJ. Treatment-specific differences were calculated using a t-test within Prism 8 (GraphPad, San Diego, CA).

### In Vitro Tubulin Polymerization Assay

A fluorescence-based porcine brain tubulin polymerization assay (Cytoskeleton, Inc., Denver, CO) was used to determine whether TDCIPP inhibits tubulin polymerization *in vitro*. The rate of polymerization was quantified in presence of 0.1% DMSO, TDCIPP (1.56–200  $\mu$ M), or nocodazole (30  $\mu$ M) according to previously described protocols.<sup>23</sup>

### Bisulfite Amplicon Sequencing (BSAS)

To test whether ciglitazone- and/or E2-mediated mitigation of TDCIPP-induced epiboly defects was associated with impacts on cytosine methylation at 2 hpf, we quantified the methylation status of five regions of interest (ROIs) that were significantly affected at 2 hpf following exposure from 0.75 to 2 hpf to 3.12  $\mu$ M TDCIPP (Table S2).<sup>11</sup> Briefly, embryos were exposed to 0.2% DMSO or 3.12  $\mu$ M TDCIPP in the presence or absence of 5  $\mu$ M ciglitazone or 5  $\mu$ M E2 from 0.75 to 2 hpf in glass petri dishes containing 10 mL of exposure solution and 30 embryos per petri dish (6 petri dishes per replicate pool). At 2 hpf, 150 surviving embryos were pooled per replicate (4 replicate pools per treatment), snap-frozen in liquid nitrogen, and stored at  $-80^{\circ}\text{C}$ . gDNA was purified and bisulfite-treated following previously described protocols<sup>11</sup>; ROIs were PCR-amplified and amplicons were purified according to previously described protocols.<sup>11</sup> gDNA quality checks were performed using an Agilent Fragment Analyzer (for gDNA) and Agilent 2100 Bioanalyzer System (DNA 1000 kit and DNA HS kit for PCR products and libraries, respectively), and all gDNA and amplicon concentrations were quantified using a Qubit 4.0 Fluorometer (ThermoFisher, Waltham, MA).

Amplicons were pooled at a concentration of 0.1 ng/amplicon, and libraries were prepared using a Nextera XT Library Prep Kit (Illumina, San Diego, CA) and paired-end sequenced on our Illumina MiniSeq Sequencing System using a 300-cycle High-Output Reagent Kit. Raw Illumina (fastq.gz) sequencing files (48 files) are available via NCBI's BioProject database under BioProject ID PRJNA553577, and a summary of sequencing run metrics are provided in Table S3 (>89.04% of reads were Q30 across all runs). Similar to previously described protocols,<sup>11</sup> downstream analysis of quality control and methylation differences were performed within Illumina's BaseSpace. Briefly, reads were aligned and duplicate reads were removed using a ROI-based enrichment manifest within MethylSeq. MethylKit was used on positions with >10X coverage to assess significant methylation differences of >1% relative to time-matched vehicle controls;  $q < 0.01$  was used to minimize false positives associated with multiple comparisons.

## Metabolomics

To assess potential effects on the embryonic metabolome, embryos were exposed to 0.2% DMSO or 3.12  $\mu\text{M}$  TDCIPP in presence or absence of 5  $\mu\text{M}$  ciglitazone from 0.75 to 6 hpf in glass petri dishes with 30 embryos per petri dish (3 petri dishes per replicate pool). At 6 hpf, 50 surviving embryos per replicate pool (4 replicate pools per treatment) were snap-frozen in liquid nitrogen. To extract metabolites, 500  $\mu\text{L}$  of ice-cold solvent (30:30:20:20 MeOH:ACN:IPA:water) was added to 50 embryos in 1.5-mL microcentrifuge tubes. Samples were then sonicated for 15 min, vortexed for 15 min, sonicated for 15 min, centrifuged at  $16,000 \times g$  at  $4^\circ\text{C}$  for 15 min, and then supernatant was transferred to glass HPLC vials. Non-polar metabolites were analyzed using a Xevo G2-XS quadrupole time-of-flight mass spectrometer (Waters Corp., Milford, MA) coupled to an H-class UPLC system (Waters Corp., Milford, MA), and polar metabolites were analyzed using a TQ-XS triple quadrupole mass spectrometer (Waters Corp., Milford, MA) coupled to an I-class UPLC system (Waters Corp., Milford, MA). Additional details are provided in Supplemental File 2.

## Results

### TPHP Mitigates TDCIPP-Induced Epiboly Defects

While neither BDCIPP nor DPHP altered TDCIPP-induced effects on epiboly (Figure S2), co-exposure to TPHP significantly mitigated the effects of TDCIPP, with an approximately 4-fold increase in the percentage of normal embryos (Figure 1A). Pre-treatments with TPHP confirmed our co-exposure results (Figure 1B), demonstrating that this protective effect was not due to decreased uptake of TDCIPP in the presence of TPHP. Moreover, based on the most potent assay hits ( $AC_{50} = 1 \mu\text{M}$ ), ToxCast-derived data also revealed that nuclear receptors (followed by transporters and cytochrome) were impacted by both TDCIPP and TPHP at low nominal concentrations (Figure 1C; Table S4).

### Nuclear Receptor Ligand Screening Reveals That Ciglitazone and E2 Mitigate TDCIPP-Induced Epiboly Defects

Based on insights from the ToxCast data, we focused on the potential role of nuclear receptors in modulating TDCIPP-induced epiboly defects as well as the protective effects of TPHP. Using a four-tiered screening strategy, we found that co-exposure with ciglitazone (a peroxisome proliferator-activated receptor  $\gamma$ , or PPAR $\gamma$ , agonist) and E2 (an estrogen receptor  $\alpha$ , or ER $\alpha$ , agonist) reliably mitigated TDCIPP-induced epiboly defects (Figure 2A) – effects that occurred in a concentration-dependent manner (Figures 2B and 2C). Similar to TPHP, the protective effect was sustained when embryos were pre-treated with ciglitazone or E2 (Figure 2D), indicating that mitigation of epiboly defects was not due to decreased uptake of TDCIPP in the presence of either ciglitazone or E2. However, unlike E2, co-exposures with two additional ER $\alpha$  agonists (EE2 and genistein) did not mitigate TDCIPP-induced epiboly defects (Figure S3). A heatmap representing transcript levels of *esr1* and *ppary* during early zebrafish development, based on a previous study<sup>24</sup>, is represented within Figure S4.



### **TDCIPP Does Not Affect Cytoskeletal Abundance within the Yolk Sac nor Cell Size within the Blastomere**

We assessed whether TDCIPP-induced epiboly defects were associated with a decrease in  $\beta$ -tubulin and/or actin abundance within the yolk sac. While TDCIPP resulted in a statistically significant increase in  $\beta$ -tubulin levels (Figure 3A), there were no significant changes in actin levels within the yolk sac (Figure 3B). Additionally, using an *in vitro* tubulin polymerization assay, TDCIPP resulted in no effects on porcine tubulin polymerization (Figure 3C). Assessment of cell area within the blastomere revealed no significant differences between DMSO- and TDCIPP-treated embryos at 5 hpf, and cell area within DMSO-treated embryos at 3 hpf was significantly higher than DMSO- and TDCIPP-treated embryos at 5 hpf (Figures 3D and 3F). Finally, TDCIPP did not adversely impact yolk syncytial nuclei (YSN) migration compared to time-matched controls (Figure 3E). Since TDCIPP did not disrupt cytoskeletal proteins in any of these assessments, further experiments with ciglitazone and E2 were not conducted.

### **E2 and Ciglitazone Mitigate TDCIPP-Induced CpG Hypomethylation**

To investigate whether the protective effects of E2 and ciglitazone were associated with a decrease in TDCIPP-induced hypomethylation, we conducted BSAS using CpG sites that were significantly impacted within our previous study.<sup>11</sup> Raw methylation data are provided within Tables S5–S7. Based on MethylKit analysis, 34 CpG sites were detected across five amplicons that were sequenced, and up to 30 sites per treatment were analyzed for differential methylation relative to DMSO controls. Interestingly, co-exposure to E2 (but not ciglitazone) significantly decreased the total number of hyper- and hypomethylated CpG sites induced by TDCIPP (Figure 4A). However, based on methylation differences across individual CpG sites, co-exposure to E2 or ciglitazone reversed the methylation status of ten and six out of 13 CpG sites, respectively, that were hypomethylated by TDCIPP (Figure 4B).

### **TDCIPP and Ciglitazone Modulate Levels of Acetylcarnitine and CDP-Choline**

We also determined whether the protective effects of ciglitazone were associated with changes in the embryonic metabolome, as ciglitazone (a PPAR $\gamma$  agonist) is an anti-diabetic thiazolidinedione that promotes lipid and glucose metabolism. All raw data for non-polar and polar lipid metabolites are provided within Tables S8 and S9, respectively. While neither TDCIPP nor ciglitazone affected non-polar metabolites, two polar metabolites (acetylcarnitine and CDP-choline) were significantly altered following exposure to TDCIPP, ciglitazone, and TDCIPP + ciglitazone ( $q < 0.05$ ). Whereas a significant increase in the relative abundance of acetylcarnitine was detected across all treatment exposures (Figure 5A), TDCIPP and ciglitazone significantly decreased and increased, respectively, the relative abundance of CDP-choline (Figure 5B). Interestingly, co-exposure to TDCIPP and ciglitazone also resulted in an increase in the relative abundance of CDP-choline compared to DMSO controls, albeit the levels were lower relative to ciglitazone-alone exposures (Figure 5B).

## Discussion

Although epiboly is critical for normal dorsoventral patterning and cell fate determination during early embryogenesis, mechanisms underlying contaminant-induced effects on epiboly within zebrafish have not been well studied to date. Within this study, using TPHP, ciglitazone, and E2, we showed that TDCIPP-induced epiboly defects may be directly associated with effects on the embryonic methylome and metabolome. Similar to TDCIPP, TPHP is ubiquitous within the indoor environment (often at higher concentrations than TDCIPP) as well as within human populations.<sup>16</sup> Within zebrafish, TPHP is known to induce cardiotoxicity, an effect that may be mediated by disruption of retinoid acid receptor signaling.<sup>22</sup> Interestingly, TPHP (but not BDCIPP nor DPHP) mitigated TDCIPP-induced epiboly defects, a finding that was unexpected since TPHP and TDCIPP both induce toxicity at later developmental stages of zebrafish development.<sup>10, 22</sup> Therefore, to investigate the potential target responsible for the protective effect of TPHP during early embryogenesis, we relied on the U.S. EPA's ToxCast data followed by a nuclear receptor ligand screen and found that ciglitazone (a PPAR $\gamma$  agonist) and E2 (an ER $\alpha$  agonist) reproducibly mitigated TDCIPP-induced epiboly defects within both co-exposure and pre-treatment experiments. Based on these results, we hypothesized that TDCIPP-induced epiboly defects may be regulated by PPAR $\gamma$  and ER $\alpha$ . Interestingly, other PPAR $\gamma$  ligands within the library (such as troglitazone and pioglitazone) or ER $\alpha$  ligands (EE2 and genistein) did not mitigate epiboly defects, suggesting that the protective effects of E2 and ciglitazone are likely independent of maternal or zygotic ER $\alpha$  and PPAR $\gamma$ . Furthermore, previous studies have shown that the levels of maternal ER $\alpha$  and PPAR $\gamma$  transcripts are non-detectable and negligible, respectively, during the first 6 h of development.<sup>24</sup> Overall, these data suggest that ciglitazone- and E2-mediated mitigation of TDCIPP-induced epiboly defects may not be driven by activation of ER $\alpha$  and PPAR $\gamma$  but, rather, related to an off-target effect that is common between both compounds. Therefore, we sought to investigate other possible mechanisms associated with the protective effects of ciglitazone and E2 on TDCIPP-induced epiboly defects.

Since epibolic abnormalities are often associated with cytoskeletal disruption,<sup>8</sup> we sought to investigate whether TDCIPP, ciglitazone, and/or E2 target this process. However, TDCIPP did not affect the abundance of yolk sac-localized actin nor  $\beta$ -tubulin *in situ* at 5 hpf. Moreover, TDCIPP did not inhibit porcine tubulin polymerization *in vitro*, nor affect the distribution of YSN – an indicator of cytoskeletal disruption *in vivo*.<sup>14</sup> Within early zebrafish development, cell division is reductive, resulting in smaller cell sizes during the course of development<sup>25</sup>; therefore, embryos with delayed development or inhibition of cell division will contain higher blastomeric cell areas. Although TDCIPP-exposed, epiboly-arrested embryos at 5 hpf were phenotypically similar to high-stage control embryos (~3 hpf) based on gross embryo morphology, the average cell area of TDCIPP-exposed embryos was comparable to time-matched controls (~5 hpf), indicating that, despite inhibition of epiboly progression, normal cell division continued within the blastomere. Overall, these data suggest that TDCIPP-induced epiboly defects were likely not associated with direct impacts on cytoskeletal reorganization or cell division. Therefore, we did not pursue further investigation with ciglitazone and E2 co-exposures.

Using restriction enzymes and bisulfite sequencing, our previous studies have shown that TDCIPP induces genome-wide CpG hypomethylation and delays remethylation during cleavage.<sup>15,20</sup> As this effect immediately precedes a sensitive window (2–3 hpf) for TDCIPP-induced epiboly defects<sup>10</sup>, these data suggest that TDCIPP-induced epiboly defects may be associated with genome-wide hypomethylation. However, in a follow-up study<sup>11</sup>, co-exposure with folic acid (a methyl donor) did not mitigate TDCIPP-induced CpG hypomethylation nor epiboly defects even though exposure to folic acid alone resulted in significant effects on methylation of CpG sites. Based on a subset of CpG sites from our prior study<sup>11</sup>, we showed here that co-exposure with E2 and ciglitazone mitigated CpG hypomethylation within TDCIPP-exposed embryos at 2 hpf. Importantly, both co-exposures reversed TDCIPP-induced hypomethylation of CpG sites within *lmo7b*, a transcript known to regulate cytoskeletal reorganization through cell-cell adhesion based on *in vitro* models<sup>26</sup> and development of cardiac muscles within zebrafish embryos.<sup>27</sup> E2 co-exposure also mitigated TDCIPP-induced hypomethylation of CpG sites within *cenpe*, a gene that regulates microtubular movements.<sup>28</sup> Although these target loci represent a small fraction of genome-wide CpG sites, our results suggest that TDCIPP-induced epiboly defects and the protective effects of E2 and ciglitazone are likely associated with genome-wide changes in the embryonic methylome prior to gastrulation.

During early embryogenesis, embryos are lipid-rich due to the presence of yolk sac-localized lipid droplets that are essential for nutrition and energy prior to commencement of independent feeding at ~7 d post-fertilization.<sup>29,30</sup> Since PPAR $\gamma$ -regulated signaling pathways modulate lipid and glucose metabolism,<sup>29</sup> we assessed whether ciglitazone-mediated mitigation of TDCIPP-induced epiboly defects were driven by alterations to the embryonic metabolome. Interestingly, while neither TDCIPP nor ciglitazone affected non-polar metabolites and the majority of polar metabolites – possibly due to a lack of direct effects on the lipid-rich yolk sac – TDCIPP and ciglitazone (as well as co-exposure to both compounds) strongly affected the relative abundance of two polar metabolites – CDP-choline and acetylcarnitine.

CDP-choline is a choline pathway intermediate involved in membrane phospholipid synthesis and stem cell proliferation.<sup>31</sup> Importantly, CDP-choline also serves as a methyl donor, and dietary choline deficiency induces cytosine hypomethylation within mammalian models.<sup>31</sup> For example, rosiglitazone (a PPAR $\gamma$  agonist similar to ciglitazone) inhibits choline-specific pathways within adult mice<sup>32</sup>, albeit the role of choline-specific pathways during early development has not been well studied. Based on the role of CDP-choline as a methyl donor, the protective effects of ciglitazone against TDCIPP-induced epiboly defects may be directly associated with the protective effects against TDCIPP-induced hypomethylation. Acetylcarnitine regulates transport of long-chain fatty acids into the mitochondria and is protective against verapamil- and ketamine-induced cardiotoxicity in zebrafish embryos<sup>33</sup>. Interestingly, zebrafish *xav* mutants (a model that is deficient in acetylcarnitine) contain increased levels of PPAR $\gamma$  protein during larval stages of development<sup>34</sup>, suggesting that PPAR $\gamma$  transcription, translation, and activation may compensate for acetylcarnitine deficiency. However, similar to CDP-choline, to our knowledge the role of acetylcarnitine in early development has not been studied, particularly during blastula and gastrula.

Our exposure regime reflects developmental stages that precede implantation and downstream development in mammals; furthermore, measurable levels of both TDCIPP and TPHP have been detected in placental samples that may impact embryos at these stages but may go undetected due to *in utero* development. Within these stages, using an *ex utero* developmental model, our data suggest that exposure to mixtures with other OPFRs (such as TPHP) can alleviate toxic effects of TDCIPP. Using rescue experiments, we showed that TDCIPP-induced epiboly defects are likely not mediated by disruption of classical mechanisms that regulate epiboly (e.g., cytoskeletal reorganization) but rather, may be directly associated with alterations in cytosine methylation and the embryonic metabolome prior to and during epiboly progression. Finally, we identified methylation dynamics within target loci (e.g., *Imo7b*) that may be used to reliably monitor the status of CpG methylation prior to TDCIPP-induced epiboly defects. Although further studies are needed to study the role of altered metabolites and specific CpG sites in driving epiboly defects, this study, using high-content screening as well as *in situ*-, *in vitro*-, mass spectrometry- and sequencing-based approaches, points to a complex interplay among nuclear receptor ligands, cytosine methylation, and the metabolome in both the induction and mitigation of epiboly defects induced by TDCIPP.

## Supplementary Material

Refer to Web version on PubMed Central for supplementary material.

## Acknowledgements:

Fellowship support was provided by UCR's Graduate Division to V.C. and S.V., and by the NRSA T32 Training Program [T32ES018827] to C.A.M. Research support was provided by a National Institutes of Health grant [R01ES027576] and the USDA National Institute of Food and Agriculture Hatch Project [1009609] to D.C.V.

## References

1. Stapleton HM; Klosterhaus S; Eagle S; Fuh J; Meeker JD; Blum A; Webster TF Detection of organophosphate flame retardants in furniture foam and U.S. house dust. *Environ. Sci. Technol* 2009, 43, 7490–5. [PubMed: 19848166]
2. Hoffman K; Butt CM; Webster TF; Preston EV; Hammel SC; Makey C; Lorenzo AM; Cooper EM; Carignan C; Meeker JD; Hauser R; Soubry A; Murphy SK; Price TM; Hoyo C; Mendelsohn E; Congleton J; Daniels JL; Stapleton HM Temporal Trends in Exposure to Organophosphate Flame Retardants in the United States. *Environ. Sci. Technol. Lett* 2017, 4, 112–118. [PubMed: 28317001]
3. Castorina R; Butt C; Stapleton HM; Avery D; Harley KG; Holland N; Eskenazi B; Bradman A Flame retardants and their metabolites in the homes and urine of pregnant women residing in California (the CHAMACOS cohort). *Chemosphere* 2017, 179, 159–166. [PubMed: 28365501]
4. Butt CM; Congleton J; Hoffman K; Fang M; Stapleton HM Metabolites of organophosphate flame retardants and 2-ethylhexyl tetrabromobenzoate in urine from paired mothers and toddlers. *Environ. Sci. Technol* 2014, 48, 10432–10438. [PubMed: 25090580]
5. Ding J; Xu Z; Huang W; Feng L; Yang F Organophosphate ester flame retardants and plasticizers in human placenta in Eastern China. *Sci. Total Environ* 2016, 554, 211–217. [PubMed: 26950635]
6. Carignan CC; Mínguez-Alarcón L; Williams PL; Meeker JD; Stapleton HM; Butt CM; Toth TL; Ford JB; Hauser R; Team ES Paternal urinary concentrations of organophosphate flame retardant metabolites, fertility measures, and pregnancy outcomes among couples undergoing in vitro fertilization. *Environ. Int* 2018, 111, 232–238. [PubMed: 29241080]

7. Hoffman K; Stapleton HM; Lorenzo A; Butt CM; Adair L; Herring AH; Daniels JL Prenatal exposure to organophosphates and associations with birthweight and gestational length. *Environ. Int* 2018, 116, 248–254. [PubMed: 29698901]
8. Lepage SE; Bruce AEE, Zebrafish epiboly: mechanics and mechanisms. *Int. J. Dev. Biol* 2010, 54 (8–9), 1213–1228. [PubMed: 20712002]
9. Dasgupta S; Vliet SM; Kupsco A; Leet JK; Altomare D; Volz DC, Tris(1,3-dichloro-2-propyl) phosphate disrupts dorsoventral patterning in zebrafish embryos. *PeerJ* 2017, 5, e4156. [PubMed: 29259843]
10. Dasgupta S; Cheng V; Vliet SMF; Mitchell CA; Volz DC Tris(1,3-dichloro-2-propyl) Phosphate Exposure During the Early-Blastula Stage Alters the Normal Trajectory of Zebrafish Embryogenesis. *Environ. Sci. Technol* 2018, 52, 10820–10828. [PubMed: 30157643]
11. Kupsco A; Dasgupta S; Nguyen C; Volz DC, Dynamic Alterations in DNA Methylation Precede Tris(1,3-dichloro-2-propyl)phosphate-Induced Delays in Zebrafish Epiboly. *Environ. Sci. Technol. Lett* 2017, 4, 367–373. [PubMed: 28993812]
12. Fu J; Han J; Zhou B; Gong Z; Santos EM; Huo X;Zheng W; Liu H; Yu H; Liu C Toxicogenomic responses of zebrafish embryos/larvae to tris (1, 3-dichloro-2-propyl) phosphate (TDCPP) reveal possible molecular mechanisms of developmental toxicity. *Environ. Sci. Technol* 2013, 47(18), 10574–10582. [PubMed: 23919627]
13. Cheng JC; Miller AL; Webb SE Organization and function of microfilaments during late epiboly in zebrafish embryos. *Dev. Dyn* 2004, 231(2), 313–23. [PubMed: 15366008]
14. Solnica-Krezel L; Driever W Microtubule arrays of the zebrafish yolk cell: organization and function during epiboly. *Development* 1994, 120 (9), 2443–55. [PubMed: 7956824]
15. Volz DC; Leet JK; Chen A; Stapleton HM; Katiyar N; Kaundal R; Yu Y; Wang Y Tris (1, 3-dichloro-2-propyl) phosphate induces genome-wide hypomethylation within early zebrafish embryos. *Environ. Sci. Technol* 2016, 50(18), 10255–10263. [PubMed: 27574916]
16. Hoffman K; Garantzios S; Birnbaum LS; Stapleton HM Monitoring Indoor Exposure to Organophosphate Flame Retardants: Hand Wipes and House Dust. *Environ. Health. Perspect* 2015, 123(2), 160–165. [PubMed: 25343780]
17. Godfrey A; Abdel-Moneim A; Sepulveda MS Acute mixture toxicity of halogenated chemicals and their next generation counterparts on zebrafish embryos. *Chemosphere* 2017, 181, 710–712. [PubMed: 28477527]
18. Macaulay LJ; Chernick M; Chen A; Hinton DE; Bailey JM; Kullman SW; Levin ED; Stapleton HM Exposure to a PBDE/OH-BDE mixture alters juvenile zebrafish (*Danio rerio*) development. *Environ. Toxicol. Chem* 2017, 36 (1), 36–48. [PubMed: 27329031]
19. Vliet SM; Ho TC; Volz DC Behavioral screening of the LOPAC1280 library in zebrafish embryos. *Toxicol. Appl. Pharmacol* 2017, 329, 241–248. [PubMed: 28623180]
20. McGee SP; Cooper EM; Stapleton HM; Volz DC Early zebrafish embryogenesis is susceptible to developmental TDCPP exposure. *Environ. Health. Perspect* 2012, 120(11), 1585. [PubMed: 23017583]
21. Volz DC; Hipszer RA; Leet JK; Raftery TD Leveraging Embryonic Zebrafish To Prioritize ToxCast Testing. *Environ. Sci. Technol. Lett* 2015, 2(7), 171–176.
22. Mitchell CA; Dasgupta S; Zhang S; Stapleton HM; Volz DC Disruption of Nuclear Receptor Signaling Alters Triphenyl Phosphate-Induced Cardiotoxicity in Zebrafish Embryos. *Toxicol. Sci* 2018, 163(1), 307–318. [PubMed: 29529285]
23. Vliet SM; Dasgupta S; Volz DC Niclosamide Induces Epiboly Delay During Early Zebrafish Embryogenesis. *Toxicol. Sci* 2018, 166(2), 306–317. [PubMed: 30165700]
24. White RJ; Collins JE; Sealy IM; Wali N; Dooley CM; Digby Z; Stemple DL; Murphy DN; Billis K; Hourlier T; Fullgrave A; Davis MP; Enright AJ; Busch-Nentwich EM A high-resolution mRNA expression time course of embryonic development in zebrafish. *Elife* 2017, 6.
25. Langley AR; Smith JC; Stemple DL; Harvey SA New insights into the maternal to zygotic transition. *Development* 2014, 141(20), 3834–41. [PubMed: 25294937]
26. Ooshio T; Irie K; Morimoto K; Fukuhara A; Imai T; Takai Y Involvement of LMO7 in the association of two cell-cell adhesion molecules, nectin and E-cadherin, through afadin and alpha-actinin in epithelial cells. *J. Biol. Chem* 2004, 279(30), 31365–73. [PubMed: 15140894]

27. Ott EB; van den Akker NM; Sakalis PA; Gittenberger-de Groot AC; Te Velthuis AJ; Bagowski CP The lim domain only protein 7 is important in zebrafish heart development. *Dev. Dyn* 2008, 237(12), 3940–52. [PubMed: 19035355]
28. Sardar HS; Luczak VG; Lopez MM; Lister BC; Gilbert SP Mitotic kinesin CENP-E promotes microtubule plus-end elongation. *Curr. Biol* 2010, 20(18), 1648–53. [PubMed: 20797864]
29. Fraher D; Sanigorski A; Mellett NA; Meikle PJ; Sinclair AJ; Gibert Y Zebrafish Embryonic Lipidomic Analysis Reveals that the Yolk Cell Is Metabolically Active in Processing Lipid. *Cell. Rep* 2016, 14(6), 1317–1329. [PubMed: 26854233]
30. Quinlivan VH; Farber SA Lipid Uptake, Metabolism, and Transport in the Larval Zebrafish. *Front. Endocrinol. (Lausanne)* 2017, 8, 319. [PubMed: 29209275]
31. Zeisel SH, Choline: critical role during fetal development and dietary requirements in adults. *Annu. Rev. Nutr* 2006, 26, 229–50. [PubMed: 16848706]
32. Pan HJ; Reifsnnyder P; Vance DE; Xiao Q; Leiter EH Pharmacogenetic analysis of rosiglitazone-induced hepatosteatosis in new mouse models of type 2 diabetes. *Diabetes* 2005, 54, (6), 1854–62. [PubMed: 15919809]
33. Guo X; Dumas M; Robinson BL; Ali SF; Paule MG; Gu Q; Kanungo J Acetyl L-carnitine targets adenosine triphosphate synthase in protecting zebrafish embryos from toxicities induced by verapamil and ketamine: An in vivo assessment. *J. Appl. Toxicol* 2017, 37(2), 192–200. [PubMed: 27191126]
34. Song Y; Selak MA; Watson CT; Coutts C; Scherer PC; Panzer JA; Gibbs S; Scott MO; Willer G; Gregg RG; Ali DW; Bennett MJ; Balice-Gordon RJ Mechanisms underlying metabolic and neural defects in zebrafish and human multiple acyl-CoA dehydrogenase deficiency (MADD). *PLoS One* 2009, 4(12), e8329. [PubMed: 20020044]



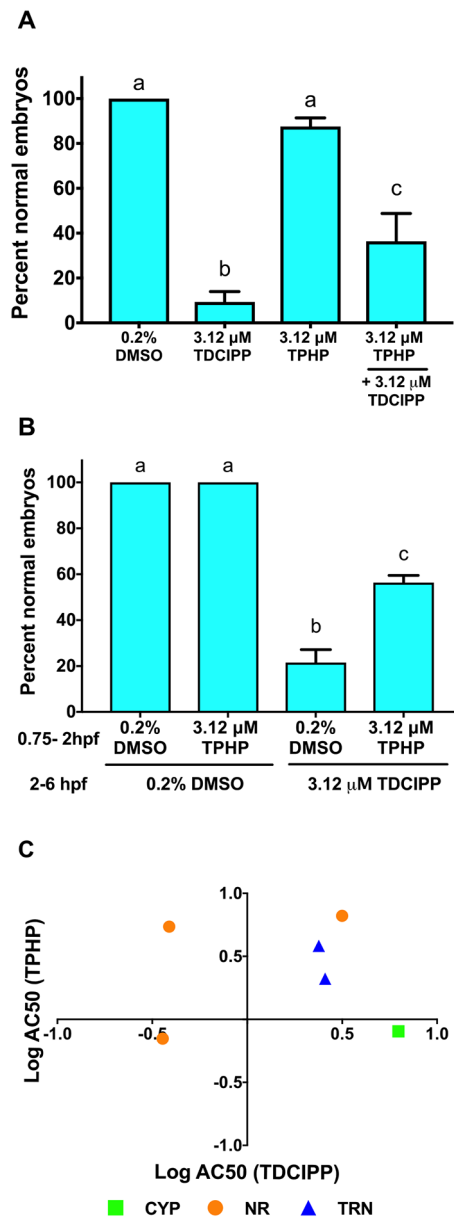


**Figure 1.**

TDCIPP-induced epiboly defects are mitigated by co-exposure (A) and pre-treatment (B) with TPHP, resulting in a higher percentage of normal embryos at 6 hpf. Each treatment group consisted of three replicate dishes with 30 live embryos per replicate dish. Bars with different letters denote statistically significant differences at  $p < 0.05$  using a one-way ANOVA followed by Tukey's post-hoc test. (C) ToxCast data representing the most potent assay hits ( $AC_{50} = 1 \mu M$ ) for both TDCIPP and TPHP. NR = nuclear receptors; TRN = transporters; and CYP = cytochrome.

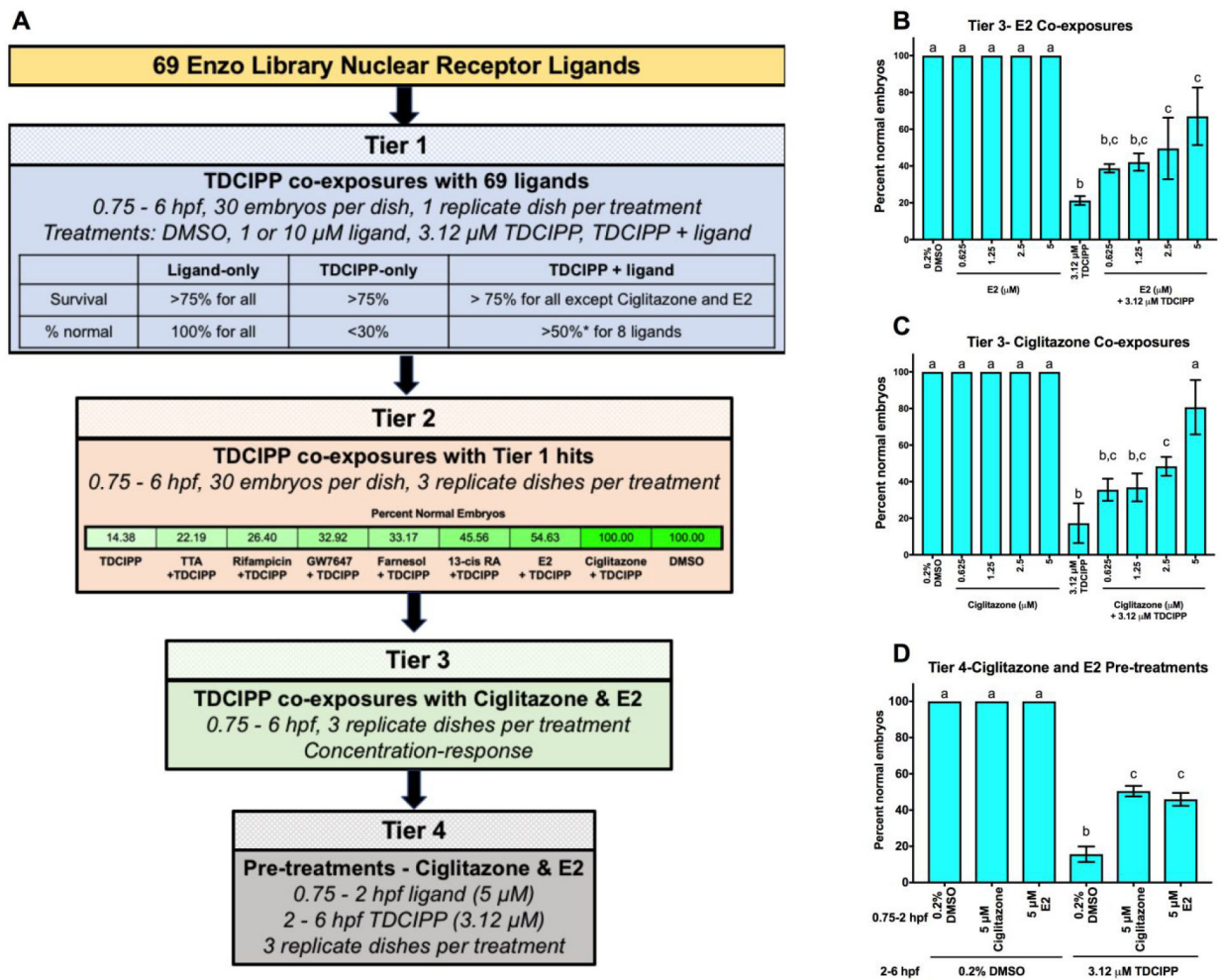


**Figure 2.** Summary of results from four-tiered screening of 69 nuclear receptor ligands in the presence or absence of TDCIPP (A). Asterisk (\*) denotes that, out of the eight ligands resulting in >50% normal embryos following co-exposure with TDCIPP, seven ligands were promoted to Tier 2 since these ligands also resulted in a >140% increase in normal embryos over corresponding TDCIPP-only treatments. Co-exposures with E2 (B) and ciglitazone (C) reveal a concentration-dependent mitigation of TDCIPP-induced epiboly defects. Pre-treatments with ciglitazone and E2 from 0.75–2 hpf followed by exposure to TDCIPP from 2–6 hpf demonstrate that the protective effects of E2 and ciglitazone are still maintained (D), albeit less potent relative to continuous E2 or ciglitazone exposure from 0.75–6 hpf.

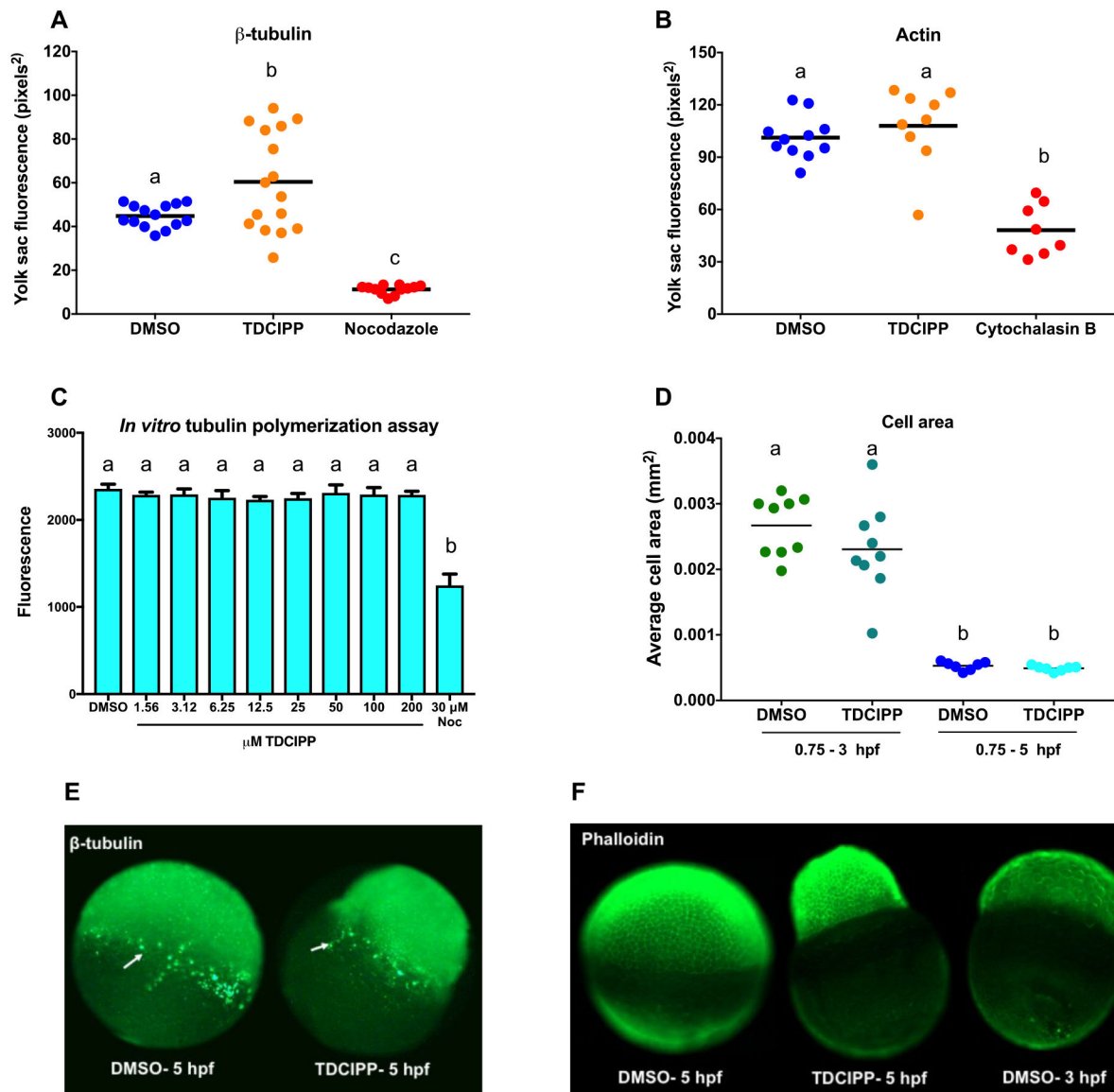


**Figure 3.**

Whole-mount immunohistochemistry reveals that TDCIPP-induced epiboly defects are not associated with reduced abundance of tubulin (A) and actin (B) within the yolk sac. Nocodazole and cytochalasin B were used as positive controls for inhibition of tubulin and actin, respectively. An *in vitro* tubulin polymerization assay (N=4 replicate wells per treatment) reveals that TDCIPP does not inhibit porcine tubulin polymerization (C). Blastomeric cell area measurements (based on the average of 15 individual cells per blastomere) reveal no effects on cell size at 5 hpf (D). Representative images from  $\beta$ -tubulin (E) and phalloidin (F) stained embryos, with white arrows pointing to yolk syncytial nuclei. Different letters denote statistically significant differences at  $p < 0.05$  using a one-way ANOVA followed by Tukey's post-hoc test.

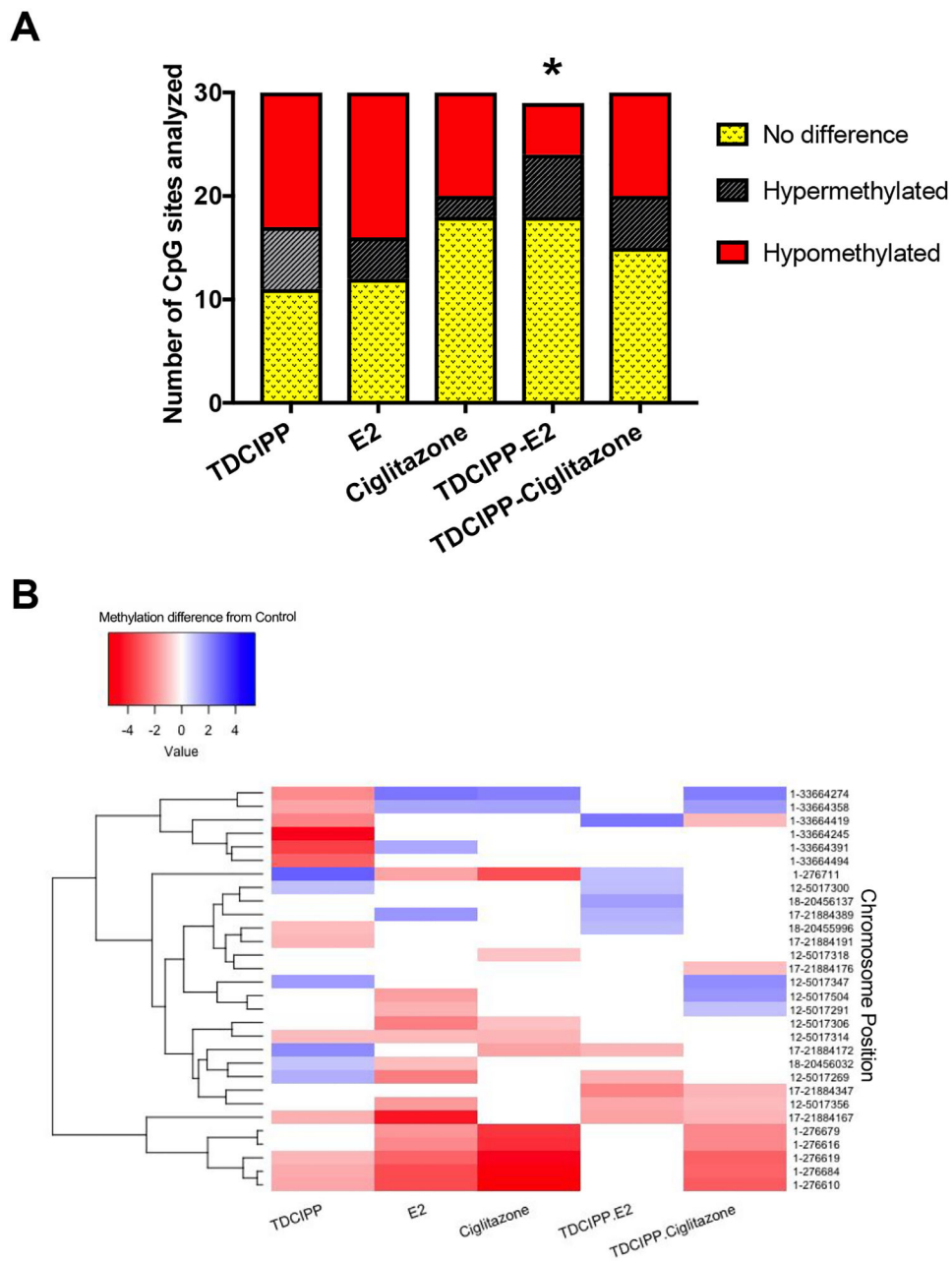


**Figure 4.**

Bisulfite amplicon sequencing of five amplicons from 2-hpf embryos exposed to TDCIPP in the presence or absence of ciglitazone or E2 from 0.75–2 hpf. Methylation status within treatment groups are relative to time-matched controls (A). Asterisk (\*) denotes a statistically significant difference (based on a Chi Squared test) in the total number of hypomethylated CpG sites ( $p < 0.05$ ) relative to TDCIPP alone. Complete linkage-based clustering of methylation differences (relative to time-matched controls) by position for all CpG sites analyzed; a methylation difference of 1% and  $q = 0.01$  were used as thresholds within MethylKit (B). All highlighted positions represent statistically significant hypomethylated CpG sites within the TDCIPP-only treatment (blue = sites localized to

*Imo7b* on chromosome 1; green = sites localized to *cenpe* on chromosome 1; and yellow = four other hypomethylated sites across three different loci localized to chromosomes 12, 17, and 18. Methylation status within each treatment were based on four independent replicates of genomic DNA.

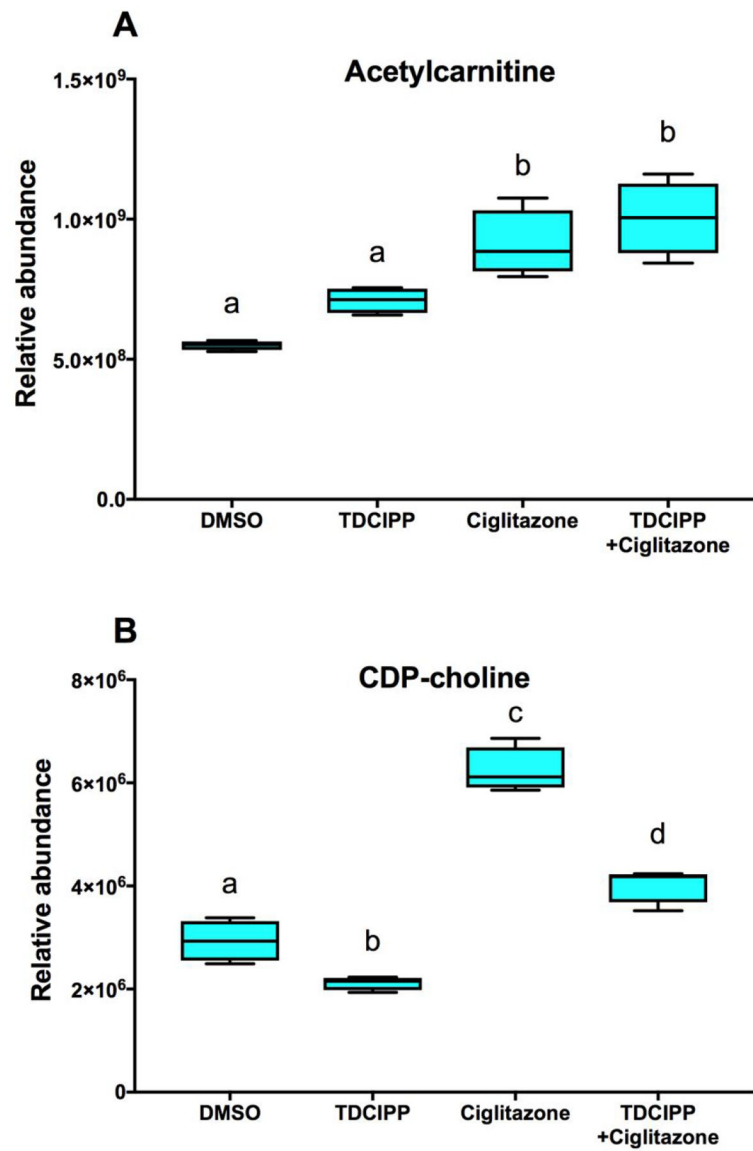


**Figure 5.** Relative abundance of acetylcarnitine (A) and CDP-choline (B) within whole embryos exposed to TDCIPP in the presence or absence of ciglitazone. Different letters denote statistically significant differences at  $p < 0.05$  using a one-way ANOVA followed by Bonferroni's post-hoc test.  $N =$  four replicates per treatment.